Property comparison of polarons in zinc-blende and wurtzite GaN/AlN quantum wells*

Zhu Jun(朱俊)[1], Ban Shiliang(班士良)[1,†], and Ha Sihua(哈斯花)[2]

[1]School of Physical Science and Technology, Inner Mongolia University, Hohhot 010021, China
[2]Department of Physics, College of Sciences, Inner Mongolia University of Technology, Hohhot 010051, China

Abstract: The properties of polarons in zinc-blende and wurtzite GaN/AlN quantum wells with Fröhlich interaction Hamiltonians are compared in detail. The energy shifts of polarons at ground state due to the interface (IF), confined (CO) and half-space phonon modes are calculated by a finite-difference computation combined with a modified LLP variational method. It is found that the two Fröhlich interaction Hamiltonians are consistent with each other when the anisotropic effect from the z-direction and the x–y plane is neglected. The influence of the anisotropy on the polaron energy shifts due to the IF phonon modes for a smaller well width or due to the CO phonon modes for a moderate well width is obvious. In addition, the built-in electric field has a remarkable effect on the polaron energy shifts contributed by the various phonon modes.

Key words: polaron; quantum well; anisotropic effect
DOI: 10.1088/1674-4926/32/11/112002 **PACC:** 7138; 7145

1. Introduction

The electron-optical-phonon interaction in quantum wells (QWs) has an important effect on the electro-optical properties in related materials and devices, and has been studied extensively during the last decades. The Fröhlich interaction Hamiltonian in zinc-blende (ZB) QWs was firstly derived by Licari and Evrard[1], and summarized by Mori and Ando[2] based on the dielectric continuum model. The polaron problem has been regarded as a basic one for using the derived electron–phonon Hamiltonian to obtain the energy spectrum of an electron with the phonon effect. The self energy or/and effective mass of a polaron in square QWs[3−7], in QWs with an electric field[8] and in asymmetric QWs[9, 10] are calculated by the LLP variational method. It suggests that there are three types of electron–phonon coupling: electron-interface (IF), electron-confined (CO) and electron-half-space (HS) modes[2, 3, 5], among them only the IF phonon frequency is dispersive. As the well width increases, the contributions to polaron energy from the three modes are very different and strongly depend on the position of the electron. The dispersion of optical phonons and the Fröhlich interaction Hamiltonian in wurtzite (WZ) QWs were deduced by Stroscio's group[11−13] using the dielectric continuum model and the uniaxial London model. All three types of phonons are dispersive and the corresponding Hamiltonians are very complicated due to the anisotropy of the dielectric mediums. The polaron properties in WZ QWs were studied by Zhu and Shi by taking into account the effect of only the IF mode[14] and all of the three modes[15]. It was found that the polaron energy and its effective mass can increase or decrease due to the anisotropy of the dielectric function and the effective band mass. Unfortunately, the authors did not discuss how the polaron energy shifts are caused by the anisotropy effect.

As mentioned by Park and Chuang[16], gallium nitride (GaN) and aluminum nitride (AlN) can exist in WZ or ZB structures depending on the growth conditions. A built-in electric field (BEF) induced by spontaneous and piezoelectric polarization exists in [0001]-oriented WZ QWs composed of GaN and AlN, whereas there is no BEF in [001]-oriented ZB QWs. The BEF, which is strong and opposite in the well and barriers, has a remarkable influence on the polaron energy[14, 15]. It is important to compare the polaron properties in ZB and WZ structures systematically. In fact, the Fröhlich interaction Hamiltonian in WZ QWs can reduce to that in ZB QWs if the dielectric anisotropy is ignored. It is the BEF that enhances the difficulty in solving the wave function of a confined electron and then the polaron problem. One can adopt a variational wave function similar to that in Ref. [8] or neglect the electric field in barriers and use an analytical Airy function[14, 15] for the electron confined in a QW. In this paper, we adopt a finite-difference computation[17] combined with a modified LLP variational method[18] to investigate the polaron energy of [001]-oriented ZB and [0001]-oriented WZ QWs.

2. Hamiltonians of polarons in ZB and WZ GaN/AlN QWs

Let us consider the QW whose geometry is given in Fig. 1. In general, the z-axis is taken to be parallel to the direction of crystal growth and the x–y plane is taken to be parallel to the interfaces. The coordinate origin is taken at the midpoint of the well. In this structure, the well material GaN is denoted by "1" and is located between $z = \pm d/2$, while the barrier material

* Project supported by the National Natural Science Foundation of China (No. 60966001), the Specialized Research Fund for the Doctoral Program of Higher Education of China (No. 20070126001), the Key Project of Natural Science Foundation of Inner Mongolia Autonomous Region (No. 20080404Zd02), and the Natural Science Doctoral Foundation of Inner Mongolia Autonomous Region (No. 2010BS0102).
† Corresponding author. Email: slban@imu.edu.cn
Received 21 January 2011, revised manuscript received 12 July 2011

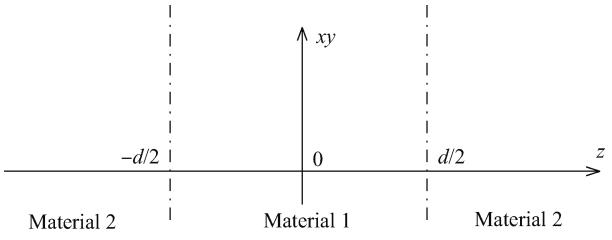

Fig. 1. A schematic geometry of GaN/AlN QWs.

AlN is denoted by "2" and fills the region $|z| > d/2$. Within the framework of the effective mass approximation, the general Hamiltonian of the polarons can be given by

$$H = H_{\rm e} + H_{\rm ph} + H_{\rm e\text{-}ph}, \tag{1}$$

with

$$H_{\rm e} = \frac{\boldsymbol{p}_\perp^2}{2m_\perp(z)} + \frac{p_z^2}{2m_z(z)} + V(z), \tag{2}$$

$$H_{\rm ph} = \sum_\lambda \sum_{\boldsymbol{k}} \hbar\omega_\lambda(\boldsymbol{k}) a_{\boldsymbol{k}}^+ a_{\boldsymbol{k}}, \tag{3}$$

and

$$H_{\rm e\text{-}ph} = \sum_\lambda \sum_{\boldsymbol{k}} \Gamma_\lambda L_\lambda(z) {\rm e}^{i\boldsymbol{q}\cdot\boldsymbol{\rho}} (a_{\boldsymbol{k}} + a_{-\boldsymbol{k}}^+), \tag{4}$$

where $m = (m_\perp, m_z)$ and $\boldsymbol{P} = (\boldsymbol{p}_\perp, p_z)$ are the effective mass and the momentum of the electron, and $V(z)$ is the potential. $a_{\boldsymbol{k}}^+ (a_{\boldsymbol{k}})$ is the creation (annihilation) operator of an optical phonon with frequency $\omega_\lambda(\boldsymbol{k})$ and wave vector $\boldsymbol{k} = (\boldsymbol{q}, k_z)$. λ refers to the IF, CO and HS optical phonon modes, respectively. There may be two types of each phonon mode, namely, symmetric (S) and antisymmetric (A) modes. Γ_λ and $L_\lambda(z)$ are the coupling coefficients of the electron–phonon interaction. It should be pointed out that the summation about $\boldsymbol{k}$ becomes $\sum\limits_{\boldsymbol{k}} \Rightarrow \sum\limits_{\boldsymbol{q}}$ since $k_z = 0$ for IF modes, $\sum\limits_{\boldsymbol{k}} \Rightarrow \sum\limits_{\boldsymbol{q}} \sum\limits_{k_{1m}}$ with $k_z = k_{1m}$ for CO modes and $\sum\limits_{\boldsymbol{k}} \Rightarrow \sum\limits_{\boldsymbol{q}} \sum\limits_{k_{2z}}$ with $k_z = k_{2z}$ for HS modes.

For an isotropic ZB QW of [001] growth-orientation, the effective mass of an electron is given by

$$m(z) = \begin{cases} m_1, & |z| \leqslant d/2, \\ m_2, & |z| > d/2, \end{cases} \tag{5}$$

with the assumption of $m_\perp(z) = m_z(z) = m(z)$.

The potential is given as

$$V(z) = \begin{cases} 0, & |z| \leqslant d/2, \\ V_0^{\rm ZB}, & |z| > d/2, \end{cases} \tag{6}$$

where $V_0^{\rm ZB}$ is the conduction band offset between the well and barriers. The phonon dispersion relations and the coupling coefficients for a ZB structure have been given in Ref. [2].

For an anisotropic [0001]-oriented WZ QW, $m_\perp(z) \neq m_z(z)$ and $\varepsilon_\perp(\omega) \neq \varepsilon_z(\omega)$. Then the effective mass of an electron is given by

$$m_{\perp,z}(z) = \begin{cases} m_{\perp,z1}, & |z| \leqslant d/2, \\ m_{\perp,z_2}, & |z| > d/2. \end{cases} \tag{7}$$

The potential is given as

$$V(z) = \begin{cases} -eF_1 z, & |z| \leqslant d/2, \\ V_0^{\rm WZ} - eF_2 z, & |z| > d/2, \end{cases} \tag{8}$$

where $V_0^{\rm WZ}$ is the conduction band offset between the well and barriers. F_i $(i = 1, 2)$ is the BEF, which can be written as[16]

$$F_1 = \frac{l(P_{{\rm pz},2} + P_{{\rm sp},2} - P_{{\rm pz},1} - P_{{\rm sp},1})}{l\varepsilon_{0,1} + d\varepsilon_{0,2}}, \tag{9}$$

and

$$F_2 = \frac{l(P_{{\rm pz},1} + P_{{\rm sp},1} - P_{{\rm pz},2} - P_{{\rm sp},2})}{L\varepsilon_{0,1} + d\varepsilon_{0,2}}, \tag{10}$$

where l and $\varepsilon_{0,i}$ are the barrier thickness and the static dielectric constant, respectively. $P_{{\rm pz},i}$ and $P_{{\rm sp},i}$ are the strain-induced piezoelectric polarization and the spontaneous polarization, respectively. The phonon dispersion relations for the WZ structure are cited from Ref. [12] while the coupling coefficients have been given in Ref. [11].

For comparison, Γ_λ and $L_\lambda(z)$ can be simplified for ZB and WZ QWs with the same numerators by using the general Lyddane-Sachs-Teller relation $\varepsilon_i(\omega) = \varepsilon_{i\infty}\frac{\omega^2-\omega_{i\rm L}^2}{\omega^2-\omega_{i\rm T}^2}$ for the ZB structure and $\varepsilon_{i\perp}(\omega) = \varepsilon_{i\infty}\frac{\omega^2-\omega_{i\perp\rm L}^2}{\omega^2-\omega_{i\perp\rm T}^2}$, $\varepsilon_{iz}(\omega) = \varepsilon_\infty\frac{\omega^2-\omega_{iz\rm L}^2}{\omega^2-\omega_{iz\rm T}^2}$ for the WZ structure. If we further set $\varepsilon_\perp(\omega) = \varepsilon_z(\omega) = \varepsilon(\omega)$, the expressions derived for the WZ structure can be consistent with that for the ZB structure.

3. Energies of polarons in ZB and WZ GaN/AlN QWs

The electron–phonon coupling constant in the bulk GaN material is estimated as 0.49[14], which is in the intermediate coupling range. We can thus use the modified LLP variational method developed by Degani and Farias[18] to calculate the energies of polarons in GaN/AlN QWs. The two unitary transformations are given by

$$U_1 = \exp\left[-i\sum_{\boldsymbol{k}} \boldsymbol{q}\cdot\boldsymbol{\rho} a_{\boldsymbol{k}} a_{\boldsymbol{k}}^+\right], \tag{11}$$

and

$$U_2 = \exp\left(\sum_{\boldsymbol{k}} f_\lambda {\rm e}^{ik_z z} a_{\boldsymbol{k}} - f_\lambda^* {\rm e}^{-ik_z z} a_{\boldsymbol{k}}^+\right), \tag{12}$$

with f_λ and its complex conjugate as variational parameters.

The wave function of the polaron is given by

$$\psi(z) = U_1 U_2 \phi(z) \left|0\right\rangle, \tag{13}$$

where $|0\rangle$ is the phonon vacuum state and $\phi(z)$ is the wave function of the electron, which can be obtained by solving the z-direction Schrödinger equation numerically. That is

Table 1. Parameters used in the computation for a ZB structure. The energy gaps are in units of eV, the effective masses in the electron rest mass m_0 and the phonon frequencies in units of cm^{-1}, respectively.

ZB	E_g	m	ω_L	ω_T	ε_∞
GaN	3.299[a]	0.19[b]	742[b]	555[b]	5.41[c]
AlN	5.400[a]	0.32[b]	902[b]	655[b]	4.46[d]

[a] Ref. [20]. [b] Ref. [21]. [c] Ref. [22]. [d] Ref. [23].

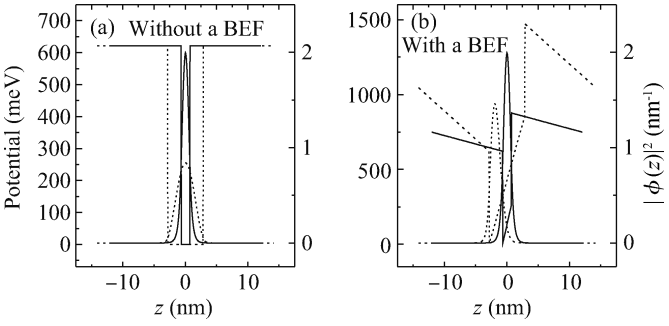

Fig. 2. Schematic potential profiles and squared wave functions of electrons at ground states for WZ GaN/AlN QWs (a) without and (b) with a BEF corresponding to $d = 0.5a_0$ (solid lines) and $d = 2a_0$ (dashed lines) . The left (right) perpendicular axes are in units of meV (nm^{-1}).

$$\left[\frac{p_z^2}{2m_z(z)} + V(z)\right]\phi(z) = E_e\phi(z). \tag{14}$$

Finally, the energy of the polaron is obtained as

$$E_{polaron} = E_e + \Delta E_\lambda. \tag{15}$$

Here the polaron energy shift can be given by

$$\Delta E_\lambda = -\sum_{\boldsymbol{k}} \frac{|\Gamma_\lambda|^2 M_\lambda^2}{\hbar\omega_\lambda + \dfrac{\hbar^2 q^2}{2m_\perp(z)} + \dfrac{\hbar^2 k_z^2}{2m_z(z)}}, \tag{16}$$

where

$$M_\lambda = \langle\phi(z)|\, e^{-ik_z z} L_\lambda(z)\,|\phi(z)\rangle\,. \tag{17}$$

4. Numerical results and discussion

All the parameters of the ZB and WZ materials used in the calculation are listed in Tables 1 and 2. The ratio of the conduction band to the valence band offset is assumed to be 6 : 4 for the ZB structure and 65 : 20 for the WZ structure[19]. The calculated results are depicted in Figs. 2–4.

Figure 2 gives specified schematic potential profiles and squared wave functions of electrons at ground state for WZ GaN/AlN QWs with and without a BEF, respectively, corresponding to different well widths d. Here the Bohr radius a_0 = 2.86 nm is chosen as a scale mark for the width of a QW. A strong penetration of electron wave functions into the barriers is indicated from the figure for a narrow QW with and without a BEF. As seen from Fig. 2(a), the squared wave functions of electrons at ground states distribute symmetrically in the QWs without a BEF. For a wider well, the quantum confinement enhances to weaken the penetration of the electron wave function into barriers. While in Fig. 2(b), both the well and barrier potentials are tilted by the BEF to enforce electrons closing the interfaces and penetrating into the barriers, although the increase of d decreases the absolute value of the BEF in wells whereas enhancing its strength in barriers.

Figure 3 shows the dispersions of phonon modes in GaN/AlN QWs. Here we only plot the high-frequency modes. It is found that the IF modes in ZB QWs exist in the frequency interval $[\omega_{2T}, \omega_{2L}]$ whereas the IF, CO and HS modes in WZ QWs exist in $[\omega_{1\perp L}, \omega_{2zL}]$, $[\omega_{1zL}, \omega_{1\perp L}]$ and $[\omega_{2zL}, \omega_{2\perp L}]$, respectively. The frequencies of IF modes in ZB QWs are slightly larger than those in WZ QWs because of the anisotropic effect. As qd increases, the frequencies of S (A) IF modes in ZB QWs decrease (increase) to reach a common limit value of about 833 cm^{-1}, while they reach about 830 cm^{-1} in WZ QWs. Furthermore, all the frequencies of CO and HS modes, including the S and A parts, increase from the lower to the upper limit with increasing qd and become weaker with an increasing quantum number m.

Figure 4 shows the polaron energy shifts as functions of d in GaN/AlN WZ QWs. Firstly, we consider the cases without a BEF in Fig. 4(a). The electron wave function is always symmetrically distributed in the QW and has a maximum at the center of the well. It extends into the well more and penetrates into the barriers less as d increases. The IF phonon potential, which has its maximum at the interfaces and rapidly decays in the well and barriers, increases with the increase of d from a small value and then decreases gradually with d. Thus, ΔE_{IF} first increases rapidly from zero to reach a maximum when d nears 1 nm, and then decreases slowly to zero with increasing d for WZ QWs without a BEF and for ZB QWs by the competition of the above two factors. The deviation caused by the anisotropic effect is obvious for smaller d and the deviation value is about 1–4 meV. ΔE_{IF} for ZB QWs is smaller than that for WZ QWs when $d < 1$ nm, but larger when $d > 1$ nm. Next, we turn to the case with a BEF. ΔE_{IF} decreases very slowly from approximately 30 meV when $d > 2$ nm since the electron, which is compelled near the left interface by the BEF and becomes easy to couple with the IF phonon potential, gradually keeps away from the interface as d increases.

However, ΔE_{CO} always increases with d, as seen in Fig. 4(b), since the electron is increasingly located at the well and easily couples with the CO phonon potential, which oscillates at the well and rapidly decays into the barriers, and thus has its maximum at the center of the well. ΔE_{CO} with a BEF is smaller than that without a BEF when $d > 8$ nm because the BEF makes the electron locate close to the left interface and weakens the coupling between the electron and the CO phonon potential. The difference between ΔE_{CO} for ZB QWs and WZ QWs without a BEF is large for a moderate d, indicating that the anisotropic effect from the z direction and the x–y plane in the quasi-2D case is obvious.

We know that the HS phonon potential oscillates at barriers and rapidly decays into the well, moreover, only a small portion of the electron wave function penetrates into the barriers, especially for a very small d. As seen in Fig. 4(c), ΔE_{HS} decreases sharply to zero for WZ QWs without a BEF and for ZB QWs due to the combination of the change in the electron wave func-

Table 2. Parameters used in the computation for a WZ structure. The energy gaps are in units of eV, the effective masses in the electron rest mass m_0 and the phonon frequencies in units of cm^{-1}, respectively.

WZ	E_g	$m_\perp$	m_z	$\omega_{\perp L}$	$\omega_{\perp T}$	ω_{zL}	ω_{zT}	$\varepsilon_{\perp\infty}$	$\varepsilon_{z\infty}$
GaN	3.43^b	0.21^b	0.19^b	741^b	559^b	734^b	532^b	5.20^e	5.39^e
AlN	6.14^b	0.33^b	0.32^b	912^b	671^b	890^b	611^b	4.30^e	4.52^e

^{b}Ref. [21]. ^{e}Ref. [24].

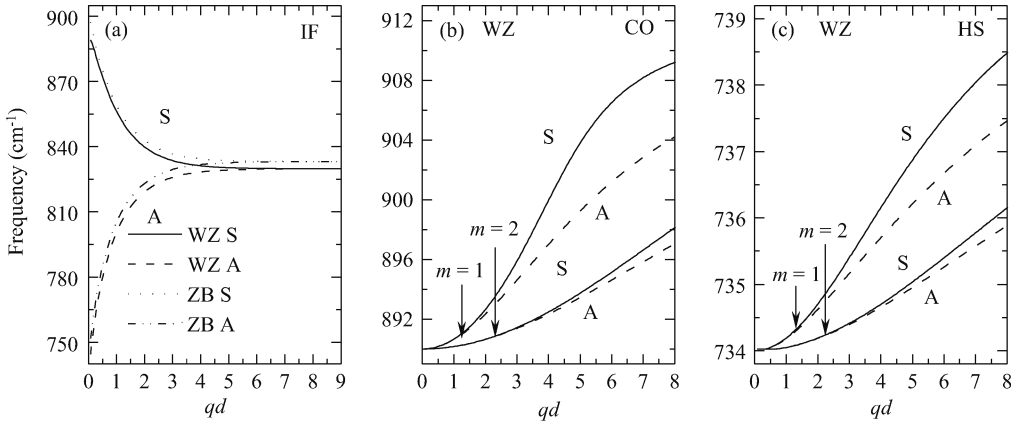

Fig. 3. Dispersion relations of (a) IF, (b) CO and (c) HS phonon modes in GaN/AlN WZ QWs. The symmetric and antisymmetric modes are denoted as S (solid lines) and A (dashed lines), respectively. The symmetric (dotted line) and antisymmetric (dash-dotted line) IF modes in ZB QWs are also plotted in (a).

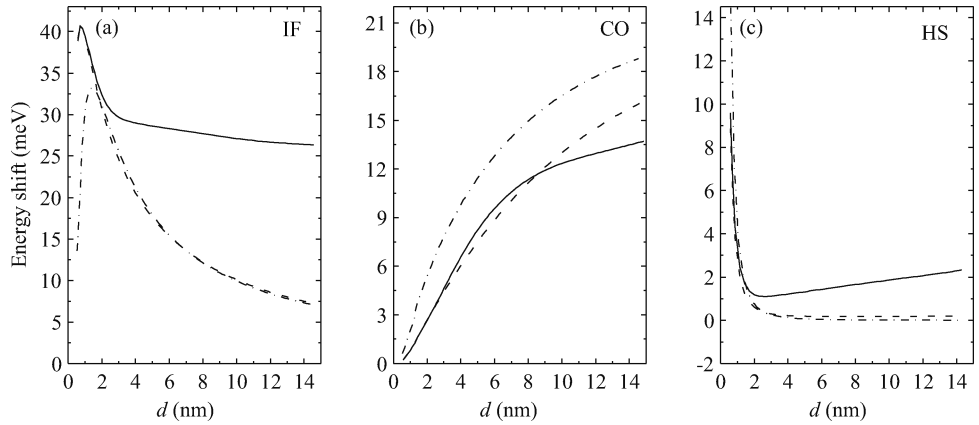

Fig. 4. Polaron energy shifts (a) ΔE_{IF}, (b) ΔE_{CO}, and (c) ΔE_{HS} as functions of the well width d for GaN/AlN WZ QWs with (solid lines) and without (dash lines) a BEF, and for ZB QWs (dash-dotted lines).

tion and the HS phonon potential. However, ΔE_{HS} decreases to a small value then gradually increases for WZ QWs with a BEF since it causes the electron wave function to be closer to the left interfaces and partly penetrates into the barriers to couple with the HS phonons. The difference between ΔE_{HS} for ZB QWs and WZ QWs without a BEF is very small (about 1 meV) even for a very small d.

It should be pointed out that our results can not completely agree with these in Ref. [15]. As d increases to a larger value, all the polaron energy shifts keep constant in Ref. [15] but they always change with d in our calculation. The main reasons include:

(1) the BEF value in Ref. [15] is taken as a constant 9.2 MV/cm but it changes as a function of the well width in our calculation;

(2) the barriers are infinite in Ref. [15] whereas the barriers are chosen to be finite in our calculation due to the adopted finite-difference numerical computation; and

(3) the factor $\exp(-ik_z z)$ in the LLP transformation in our calculation is different from that in Ref. [15].

5. Conclusion

In conclusion, we compare the polaron properties in ZB and WZ QWs with the Fröhlich interaction Hamiltonian. It is found that the two Fröhlich interaction Hamiltonians are consistent with each other if the anisotropic effect from the z direction and the x–y plane is neglected. However, the influences from the anisotropic effect on the polaron energy shifts ΔE_{IF} for a smaller d and ΔE_{CO} for a moderate d are obvious. The

BEF has a remarkable effect on the polaron energy shifts contributed by the three various phonon modes. The current work is useful to further study the phonon-assisted electro-optical properties in wurtzite semiconductor low-dimensional structures.

References

[1] Licari J J, Evrard R. Electron–phonon interaction in a dielectric slab: effect of the electronic polarizability. Phys Rev B, 1977, 15: 2254

[2] Mori N, Ando T. Electron-optical-phonon interaction in single and double heterostructures. Phys Rev B, 1989, 40: 6175

[3] Hai G Q, Peeters F M, Devreese J T. Electron-optical-phonon coupling in GaAs/$Al_xGa_{1-x}As$ quantum wells due to interface, slab, and half-space modes. Phys Rev B, 1993, 48: 4666

[4] Zheng R S, Ban S L, Liang X X. Effects of interface and bulk optical phonons on polarons in a quantum well. Phys Rev B, 1994, 49: 1796

[5] Lu T Q, Zheng Y S. Polaron properties in quantum wells. Phys Rev B, 1996, 53: 1438

[6] Mora-Ramos M E, Contereras-Solorio D A. The polaron in a GaAs/AlAs quantum well. Physica B, 1998, 253: 325

[7] Li T Z, Wang K L, Yang J L, et al. A new variational method for the coupling system of polaron in a quantum well. Phys Status Solidi B, 1999, 212: 271

[8] Chen C Y, Liang S D, Li M. A polaron in a quantum well within an electric field. J Phys: Condens Matter, 1994, 6: 1903

[9] Shi J J, Zhu X Q, Liu Z X, et al. Polaron effects in asymmetric semiconductor quantum-well structures. Phys Rev B, 1997, 55: 4670

[10] Zhu X Q, Shi J J, Liu Z X, et al. Energy and effective mass of a polaron in asymmetric semiconductor quantum well structures. Z Phys B, 1997, 102: 207

[11] Lee B C, Kim K W, Stroscio M A, et al. Optical-phonon confinement and scattering in wurtzite heterostructures. Phys Rev B, 1998, 58: 4860

[12] Komirenko S M, Kim K W, Stroscio M A, et al. Dispersion of polar optical phonons in wurtzite quantum wells. Phys Rev B, 1999, 59: 5013

[13] Chen C, Dutta M, Stroscio M A. Confined and interface phonon modes in GaN/ZnO heterostructures. J Appl Phys, 2004, 95: 2540

[14] Zhu Y H, Shi J J. Polaron effects due to interface optical-phonons in wurtzite GaN/AlN quantum wells. Phys Status Solidi B, 2005, 242: 1010

[15] Zhu Y H, Shi J J. Effects of built-in electric field on polarons in wurtzite GaN/AlN quantum wells. Physica E, 2009, 41: 746

[16] Park S H, Chuang S L. Comparison of zinc-blende and wurtzite GaN semiconductors with spontaneous polarization and piezoelectric field effects. J Appl Phys, 2000, 87: 353

[17] Zhu J, Ban S L, Ha S H. Binding energies of excitons in strained [0001]-oriented wurtzite AlGaN/GaN double quantum wells. Phys Status Solidi B, 2011, 248: 384

[18] Degani M H, Farias G A. Anisotropic polarons near interfaces of polar semiconductors. Phys Rev B, 1990, 41: 3572

[19] Nardelli M B, Rapcewicz K, Bernholc J. Strain effects on the interface properties of nitride semiconductors. Phys Rev B, 1997, 55: R7323

[20] Vurgaftman I, Meyer J R. Band parameters for nitrogen-containing semiconductors. J Appl Phys, 2003, 94: 3675

[21] Wu J Q. When group-III nitrides go infrared: new properties and perspectives. J Appl Phys, 2009, 106: 011101

[22] Karch K, Wagner J M, Bechstedt F. *Ab initio* study of structural, dielectric, and dynamical properties of GaN. Phys Rev B, 1998, 57: 7043

[23] Karch K, Bechstedt F. *Ab initio* lattice dynamics of BN and AlN: covalent versus ionic forces. Phys Rev B, 1997, 56: 7404

[24] Wagner J M, Bechstedt F. Properties of strained wurtzite GaN and AlN: *ab initio* studies. Phys Rev B, 2002, 66: 115202